

Rydberg six-wave mixing spectrum under ionized environment variation

Yinglong Diao(刁赢龙), Haoliang Hu(胡浩亮), Xiaofei Li(李小飞), Zhibo Li(李治博), Feitong Zeng(曾非同), Yanbin Chen(陈焱斌), and Shuhang You(游书航)

Citation: Chin. Phys. B, 2026, 35 (**2**): 023201. DOI: 10.1088/1674-1056/adf318
http://cpb.iphy.ac.cn; http://iopscience.iop.org/cpb

What follows is a list of articles you may be interested in

Microwave field sensor based on cold cesium Rydberg three-photon electromagnetically induced spectroscopy

Yuan-Yuan Wu(吴圆圆), Yun-Hui He(何云辉), Yue-Chun Jiao(焦月春), and Jian-Ming Zhao(赵建明)
Chin. Phys. B, 2024, 33 (**11**): 113201. DOI: 10.1088/1674-1056/ad7579

Atom-based power-frequency electric field measurement using the radio-frequency-modulated Rydberg spectroscopy

Weixin Liu(刘伟新), Linjie Zhang(张临杰), and Tao Wang(汪涛)
Chin. Phys. B, 2023, 32 (**5**): 053203. DOI: 10.1088/1674-1056/aca6db

Electric field intensity measurement by using doublet electromagnetically induced transparency of cold Rb Rydberg atoms

Ting Gong(宫廷), Shuai Shi(师帅), Zhonghua Ji(姬中华), Guqing Guo(郭古青), Xiaocong Sun(孙小聪), Yali Tian(田亚莉), Xuanbing Qiu(邱选兵), Chuanliang Li(李传亮), Yanting Zhao(赵延霆), and Suotang Jia(贾锁堂)
Chin. Phys. B, 2023, 32 (**10**): 103202. DOI: 10.1088/1674-1056/acf120

High-precision three-dimensional Rydberg atom localization in a four-level atomic system

Hengfei Zhang(张恒飞), Jinpeng Yuan(元晋鹏), Lirong Wang(汪丽蓉), Liantuan Xiao(肖连团), and Suo-tang Jia(贾锁堂)
Chin. Phys. B, 2021, 30 (**5**): 053202. DOI: 10.1088/1674-1056/abd46f

Dissipative preparation of multipartite Greenberger-Horne-Zeilinger states of Rydberg atoms

Chong Yang(杨崇), Dong-Xiao Li(李冬啸), and Xiao-Qiang Shao(邵晓强)
Chin. Phys. B, 2021, 30 (**2**): 023201. DOI: 10.1088/1674-1056/abd755

Rydberg six-wave mixing spectrum under ionized environment variation

Yinglong Diao(刁赢龙)[1], Haoliang Hu(胡浩亮)[1], Xiaofei Li(李小飞)[1], Zhibo Li(李治博)[1], Feitong Zeng(曾非同)[1], Yanbin Chen(陈焱斌)[2], and Shuhang You(游书航)[1,†]

[1] *China Electric Power Research Institute Wuhan Branch, Wuhan* 430074, *China*
[2] *Wuhan Yunheng Technology Co., Ltd., Wuhan* 430056, *China*

(Received 11 May 2025; revised manuscript received 26 June 2025; accepted manuscript online 23 July 2025)

This paper presents the high-order nonlinear spectrum of six-wave mixing (SWM) influenced by ionizing Rydberg atom environment in rubidium thermal vapor. The experimentally measured transmitted SWM signals reveal significant spectrum shifts and novel regularities, providing nonlinear spectrum insights into the ionization characteristics of Rydberg atoms. The detailed spectrum variations with increasing ion density are presented, paving the way for multi-wave mixing distribution of plasma and demonstrating SWM's potential as a tool for measuring the electric field induced by the ionization process.

Keywords: Rydberg atoms, six-wave mixing (SWM), electric field measurement

PACS: 32.80.Rm, 42.65.Hw, 52.70.–m, 32.60.+i

DOI: 10.1088/1674-1056/adf318 **CSTR:** 32038.14.CPB.adf318

1. Introduction

Rydberg atomic spectroscopy in the ionic environment plays an important role in astrophysics research[1] and plasma diagnosis.[2] The study of the ionization process of Rydberg atoms provides many useful parameters for astrophysics, which are essential for understanding physical phenomena in the universe.[3] It is crucial for providing accurate parameters, promoting the development of measurement technology, and broadening the scope of plasma research.[4] For example, studying the collision process between ions and Rydberg atoms in the celestial environment can provide many useful parameters for astrophysics, such as the characteristic spectral lines emitted after charge transfer, which are important to determine the abundance of matter.[5] By analyzing the spectra of Rydberg atoms, the spectral line shape and atomic kinetics in plasma have been simulated, which is essential for understanding the physical state and dynamic processes of the plasma.[6] The unique properties of Rydberg atoms make them useful for high-precision spectroscopy, which is a sophisticated measurement tool to detect microwaves and radio waves, as well as to analyze the strength and properties of electromagnetic fields.[7]

Rydberg atom is easily affected by the external electric field because of its large principal quantum number n and weak binding force between its outermost electron and the nucleus.[8] When Rydberg atoms are placed in a strong electric field, their energy levels shift; this phenomenon is known as the Stark effect.[9] For decades, the intensity and frequency of the electric field have been accurately measured by analyzing the frequency shift of the electromagnetically induced transparency (EIT) spectrum of Rydberg atoms by modulating the amplitude of the radio frequency electric field using a power frequency electric field.[10] In contrast to EIT, six-wave mixing (SWM), a fifth-order nonlinear process, can be achieved in the EIT window using five excitation beams.[11] SWM spectrum has a narrower line width than EIT, making it more sensitive to the electric field.[12] The ionization of Rydberg atoms can produce an electric field. Thus, once the SWM process occurs in ionization, it will be influenced by the electrical field caused by the ionization environment. Field measurement technology is being extended to the Rydberg SWM domain, which has a wide range of applications in electric power, industrial production, and scientific research. Rydberg atomic SWM spectra can play a fundamental role in the measurement of electric fields and provide important technical support for research and applications.

In this paper, we experimentally obtain SWM spectra of Rydberg states in a collective ensemble of rubidium thermal vapors and study their evolution in an ionization environment. By adjusting experimental parameters to change ionization density, ionization-induced Rydberg SWM spectrum characteristics are observed at room temperature. Spectrum shifts and broadening are presented, demonstrating their potential use in detecting electric fields induced by ionization.

[†]Corresponding author. E-mail: youshuhang@outlook.com

© 2026 Chinese Physical Society and IOP Publishing Ltd. All rights, including for text and data mining, AI training, and similar technologies, are reserved.

2. Theoretical model and experimental scheme

To achieve the Rydberg SWM process, an inverted Y-type four-level atomic system is used in our experiment. As shown in Fig. 1(a), ground states $5S_{1/2}$, $F = 3(|0\rangle)$ and $5S_{1/2}$, $F = 2(|3\rangle)$ are excited to the first excited state $5P_{3/2}$ $(|1\rangle)$, which is then excited to the second high-lying Rydberg state $nD_{5/2}$ $(|2\rangle)$ of ^{85}Rb. As illustrated in Fig. 1(a), four Gauss-type laser beams from three commercial external cavity diode lasers (DLs) with frequency-stabilized devices are coupled into the appropriate transitions. The optical path of the experiment is shown in Fig. 1(b). A weak laser beam $\boldsymbol{E}_1$ (with wavelength 780.24 nm, diameter 0.8 mm, frequency ω_1, and wave vector $\boldsymbol{k}_1$) from DL1 probes the lower transition $|0\rangle$ to $|1\rangle$, while a pair of coupling beams $\boldsymbol{E}_3$ (780.23 nm, ω_3, $\boldsymbol{k}_3$) and $\boldsymbol{E}_3'(\omega_3, \boldsymbol{k}_3')$, derived from the same DL3 with a small angle between them both with diameter 1 mm, connect another lower transition $|3\rangle$ to $|1\rangle$. By frequency doubling DL2 at 960 nm with a periodically poled KTP crystal in an external ring resonator, 480-nm laser $\boldsymbol{E}_2(\omega_2, \boldsymbol{k}_2)$ is obtained to excite thermal Rb atoms from level $|1\rangle$ to Rydberg states $|2\rangle$. The strong beam $\boldsymbol{E}_2$ (diameter 1 mm) is added to the beam $\boldsymbol{E}_3$ (in the same direction), which then counter-propagates with beam $\boldsymbol{E}_1$. Before the cell, two identical lenses (L1 and L2, respectively) with focal lengths of 500 mm focus all of the beams, which cross at a single point within the cell. The heater tape encased with μ-metal heats the 5-cm-long rubidium cell to adjust its temperature, allowing control over the density of the ground atoms. The atomic density of ground state can be calculated by measuring the temperature and pressure of the gas cell and combining them with the state equation.

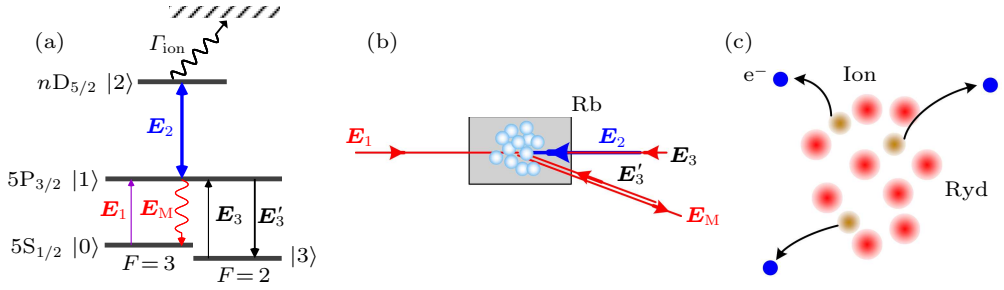


Fig. 1. Model and experimental setup. (a) An inverted Y-type four-level atomic system in ^{85}Rb atom for experimental processes, which includes hyperfine states $F = 3(|0\rangle)$ and $F = 2(|3\rangle)$ of the ground state $5S_{1/2}$, a first excited state $5P_{3/2}$ $(|1\rangle)$, and a highly-excited Rydberg state $nD_{5/2}$ $(|2\rangle)$. (b) The laser beam propagation geometry in the experiment. (c) Simple ionization process simulation of Rydberg (Ryd) atoms.

This excitation process involves two types of multi-wave mixing (MWM) processes. First, without beams $\boldsymbol{E}_2$, a Four-wave mixing (FWM) process with the phase-matching condition (PMC) $\boldsymbol{k}_{\rm FWM} = \boldsymbol{k}_1 + \boldsymbol{k}_3 - \boldsymbol{k}_3'$ occurs in the Λ-type three-level subsystem $|0\rangle \leftrightarrow |1\rangle \leftrightarrow |3\rangle$. Then, beam $\boldsymbol{E}_2$ participation and an EIT-assisted SWM signal $\boldsymbol{E}_{\rm SWM}$ with the PMC $\boldsymbol{k}_{\rm SWM} = \boldsymbol{k}_1 + \boldsymbol{k}_2 - \boldsymbol{k}_2 + \boldsymbol{k}_3 - \boldsymbol{k}_3'$ can be observed in $|0\rangle \leftrightarrow |1\rangle \leftrightarrow |2\rangle \leftrightarrow |3\rangle$. This configuration builds coherence in each corresponding three-level subsystem, enhancing the efficiency of the MWM process.[13,14] These MWM signals have the same emitting direction (opposite to the direction of $\boldsymbol{E}_3'$, as shown in Fig. 1(b)), which can be identified by tuning the frequency detuning of various incident beams, and are detected by an avalanche photodiode detector (APD). The APD receives the SWM signal through the front amplifier and then finally transmits to the oscilloscope, where it can be observed SWM spectrum. It is specifically known as the Rydberg signal with particular features, and it is associated with the Rydberg state $|2\rangle$. According to the energy system and Liouville pathways, considering the dressing effect of the generated EIT and SWM[15] and the Doppler effect (kv), the first-order and fifth-order density matrix elements with all four beams on are as follows:

$$\rho_{10\rm D}^{(1)} = \mathrm{i}\,|G_1|/[d_1 + |G_2|^2/d_2], \tag{1}$$

$$\rho_{10}^{(5)} = \mathrm{i}G_1\,|G_2|^2\,|G_3|^2/[d_1 + |G_2|^2/d_2]^3 d_2 d_3, \tag{2}$$

where $d_1 = \Gamma_{10} + \mathrm{i}(\Delta_1 + k_1 v)$, $d_2 = \Gamma_{20} + \mathrm{i}\Delta_1 + \mathrm{i}\Delta_2 + \mathrm{i}(k_1 v - k_2 v)$, $d_3 = \Gamma_{30} + \mathrm{i}\Delta_1 + \mathrm{i}\Delta_3 + \mathrm{i}(k_1 v - k_3 v)$, frequency detuning $\Delta_i = \Omega_i - \omega_i$ ($\Omega_{\rm i}$ is the resonance frequency of the transition driven by $\boldsymbol{E}_i$), $G_i = \mu_{ij}\boldsymbol{E}_i/\hbar$ is the Rabi frequency of the optical field, Γ_{n0} are the decay rates of $|n\rangle$ (n = 1, 2, or 3) and $|0\rangle$, and v is the relative velocity between atoms and corresponding light field. $\rho_{10}^{(5)}$ is the Rydberg SWM density matrix element that can determine the intensity of Rydberg SWM signals. Rydberg interaction and ionization can generate a blockade effect,[16] which suppresses the excitation state and shifts the energy level, yielding ionization during the experimental process due to their significant polarization and collisions with electrons, ions, or other atoms. The atom ionizes when its electrons are removed, as shown in Fig. 1(c). Rydberg atoms are influenced by the blockade effect and sensitive to such surroundings due to their large dipole moment and high polarizability. When the interaction and ionization effects are changed, a frequency shift and a relaxation rate will change. The blockade causes the energy level to be excited to the Rydberg state shift to $\Delta_2 + \Delta_{\rm b}$. The ionization

causes an effective Rydberg atom number-dependent detuning of the $\boldsymbol{E}_2$ field $\Delta_2 \to \Delta_2 + \Delta_s$ and the corresponding decay rate $\Gamma_{20} \to \Gamma_{20} + \Gamma'$.[17] Specifically, positive ions and electrons can produce an inhomogeneous local electric field in the vicinity of the atomic vapor. Δ_b can be calculated through Ref. [18], which, together with the local electric field, affects Rydberg atoms, causing Rydberg level shift and a change in relaxation rate. When the electron density and the positive ion density are assumed to be identical, the induced density of charged particles N_C provides both parameters. For obtaining Δ_s, the following rate equations can be solved to determine the relation between the density of charged particles and Rydberg atomic density[19]

$$\dot{N}_{Ryd} = -N_{Ryd}N_g\sigma_g\bar{v} - N_{Ryd}N_{Ryd}\sigma_{Ryd}\bar{v}' + R_{exc}, \quad (3)$$

$$\dot{N}_C = -N_{Ryd}N_g\sigma_g\bar{v} - N_{Ryd}N_{Ryd}\sigma_{Ryd}\bar{v}' - N_C\Gamma_d, \quad (4)$$

where σ_g is the cross-section of atomic collisions in the Rydberg-ground state, N_{Ryd} and N_C are the Rydberg atom density and induced density of the charged particles, respectively. N_g is the ground-state atomic density, $\bar{v}$ is the average relative velocity of ground-state atoms and colliding Rydberg atoms, and $\bar{v}'$ is the mean relative velocity of Rydberg atoms colliding with other Rydberg atoms, σ_{Ryd} and is the geometric cross-section of collisions between Rydberg atoms.[20,21] The estimated value of σ_g is approximately $0.06\sigma_{Ryd}$, where $\sigma_{Ryd} = \pi(a_0^2 n^{*4})$[22] ($a_0$ is the Bohr radius) is the geometric cross-section of the Rydberg state determined by the effective principal quantum number n^*. Rydberg component in the superposition dark state of EIT is described as $R_{exc} = G_1^2/(G_1^2+G_2^2)\cdot N_g G_1 G_2/\Delta_2 + \Delta_1$. In Eq. (4), Γ_d represents charged particles recombination and decay rate, which can be expressed as $\Gamma_d = \Gamma_{20} + 2N_g\sqrt{8K_BT/(\pi m_e)}\sigma_r\rho_c$. Γ_{20} is assume to be 0.25 MHz. The second term of Γ_d can be approximated as $2\Gamma_r$, which explains how ions and electrons can recombine to form neutral particles. K_B is the Boltzmann constant, m_e is the electron mass, ρ_c is the charged particles population, with $\rho_c \approx 1$ is assumed theoretically. Kramer's formula can be used to determine the expected value of σ_r in a semiclassical treatment.[23] Since $2\Gamma_r$ is negligible in comparison to the ion diffusion rate of 0.25 MHz, it can be disregarded.

The local electric field can be defined as[24,25] $\varepsilon = 2.603\,|e|/(4\pi\varepsilon_0)\cdot N_C^{2/3}$ using the computed density of charged particles, where ε_0 is the vacuum dielectric constant and e is the electron charge. Secondorder perturbation theory provides the Stark shift of the Rydberg state in low electric fields as $\Delta_S = -(1/2)\alpha\varepsilon^2$,[26] where α is the Rydberg state's atomic polarizability, which can be computed by consulting Ref. [18]. Rydberg level shift varies with charged particle density as

$$\Delta_S = -\frac{1}{2}\alpha\left(\frac{2.603\cdot|e|}{4\pi\varepsilon_0}\cdot N_C^{2/3}\right)^2. \quad (5)$$

The Rydberg energy level shift Δ_S calculated using Eq. (5) is shown in Fig. 4(c), which can be as a theoretical standard to estimate energy level shift caused by electric field.

3. Results and discussion

Rydberg SWM spectra under low and high densities are presented in Fig. 2. Different scanning methods are shown in Figs. 2(a) and 2(b), respectively. Each peak in the figure represents Rydberg SWM signals. Zero detuning of Δ_1 and Δ_2 is identical to the Rb $5S_{1/2}$ $(F=3) \to 5P_{3/2} \to 37D_{5/2}$ cascade resonance. The spectral lines on the right side of Fig. 2(a) are the baseline of FWM. The experimental results show a clear spectrum peak shift. The frequency shift value in the high-density case is roughly 100 MHz, which is attributed to three factors: the Doppler effect, Rydberg interaction, and ionization. In our experiment, the 780 nm and 480-nm lasers are oppositely incident, making a large Dopplerfree region, resulting in a weak frequency shift. When it is a dipole–dipole interaction, which is proportional to $1/R_3$, the Rydberg level shift for the $37D_{5/2}$ state can be calculated within a short-distance range using Rydberg atomic density.[18] In the long-distance range, the interaction is Van der Waals, which is proportional to $1/R_6$. Therefore, the Rydberg level shift due to Rydberg interaction is smaller than our measured values. According to the conclusion of reference,[27] it is impossible to cause a Rydberg level shift of several hundred MHz. The remaining frequency shift value indicates that the electric field generated by the collisions of Rydberg atoms causes the Rydberg energy level shift Δ_S. The variation in Δ_S alters $\rho_{10}^{(5)}$, causing shifts in SWM spectra due to the high density of atoms colliding with one another, which creates ions. According to our measurements, the Rydberg level shift caused by the interaction of Rydberg atoms and ionization is the most important factor. To further investigate SWM spectrum evolution under an ionized environment, detailed spectral variations with density changes are presented below.

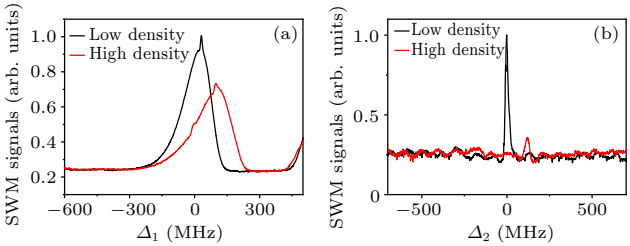


Fig. 2. (a) SWM spectrum in the two atomic densities when scanning Δ_1. (b) SWM spectrum in the two atomic densities when scanning Δ_2. Low density is 1.0×10^{10} cm^{-3}, whereas high density is 1.0×10^{11} cm^{-3}.

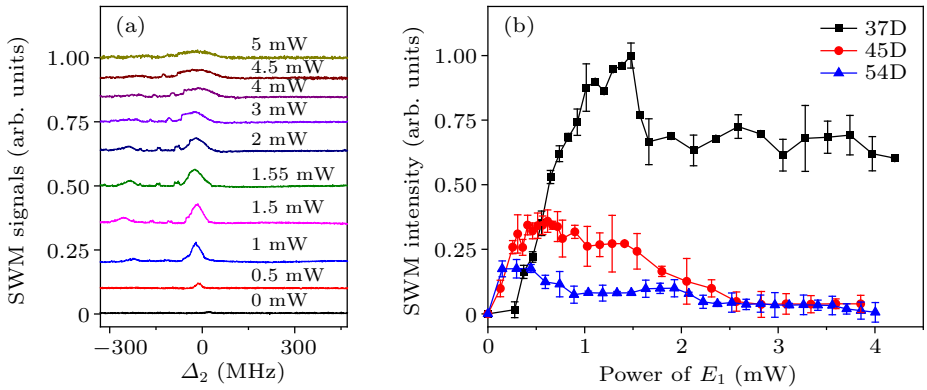


Fig. 3. The dependence of Rydberg SWM signal intensities on power and Δ_2. (a) The measured $37D_{5/2}$ Rydberg SWM spectra *versus* Δ_2 for different probe field powers. (b) Probe power dependence curves of different Rydberg states $37D_{5/2}$, $45D_{5/2}$, and $54D_{5/2}$. The error bars in panel (b) represent the standard deviation of repeated measurements.

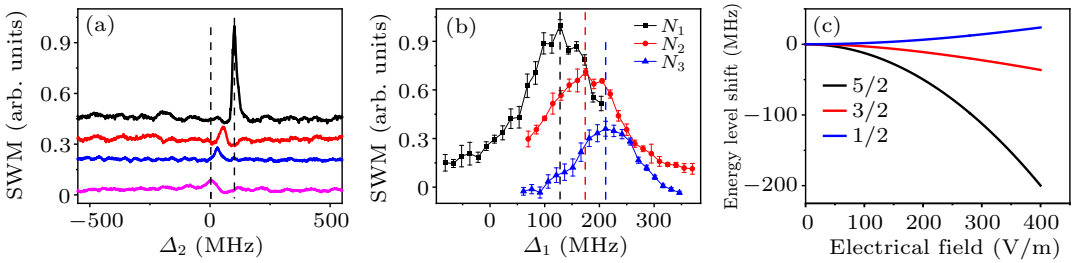


Fig. 4. (a) The measured SWM signals via scanning Δ_2 at different Δ_1 from top to bottom: −80 MHz, −40 MHz, −20 MHz, and 0 MHz. (b) The intensity dependence curves of SWM signals through measuring intensity resemble (a) at different atomic densities: $N_1 = 1.0 \times 10^{11}$ cm^{-3}, $N_2 = 1.0 \times 10^{12}$ cm^{-3}, and $N_3 = 5.0 \times 10^{12}$ cm^{-3}. (c) Variation of calculated energy level shift *versus* electrical field intensity, when $m_j = 5/2$, 3/2, or 1/2. The error bars in panel (b) represent the standard deviation of repeated measurements.

Since the ionization process is more likely to occur in a high-density environment, some parameters can be varied to control the density of Rydberg atoms. In the following, considering that laser powers and principal quantum number have a significant effect on the density of Rydberg atoms, SWM signals are changed by the power of $\boldsymbol{E}_1$ for different n values are presented. The $37D_{5/2}$ Rydberg state spectra are shown in Fig. 3(a), indicating that the intensity of SWM signals increases when $\boldsymbol{E}_1$ power increases to 1.5 mW, then decreases, and the line width of the spectrum becomes wider.

According to Eq. (2), SWM signals should increase with increasing power. In fact, Rydberg interaction becomes strong and collisions become more intense as the power increases, producing a large number of ions. Rydberg interaction shifts the SWM signals. A large number of ions generate an electric field, which not only shifts but also broadens SWM signals, as shown in Fig. 3(a). These phenomena are easier to understand theoretically; the interaction and the presence of a number of ions result in $\Delta_2 \to \Delta_2 + \Delta_b + \Delta_s$, with a corresponding decay rate $\Gamma_{20} \to \Gamma_{20} + \Gamma'$. The change of $\Delta_b + \Delta_s$ causes the SWM spectrum peak to shift and Γ' makes the SWM spectrum weaker. The linewidth increases due to large excitation power and the collision of a large number of ions and atoms. Theoretically, the energy level structure, transverse relaxation rate, and energy level lifetime all play a role in determining the minimal line-width of SWM. However, the line-width of SWM can be influenced by many factors, such as excitation power, transition probability, and atomic collisions. According properties of Rydberg interaction, the larger the principal quantum number, the stronger the interaction, the easier the ionization, and the greater the influence of the electric field. It is expected that the larger the principal quantum number, the better the spectral shift for detecting changes in the ionizing environment. However, as shown in Fig. 3(b), SWM spectra of $45D_{5/2}$ and $54D_{5/2}$ are very weak due to a large transition dipole moment and easier ionization. The weakest SWM spectrum is not the best choice for measuring the ionizing electric field because of its energy level shift.

Therefore, the $37D_{5/2}$ Rydberg state is chosen to investigate spectrum shift variation for detecting the ionization electric field. Figure 4(a) shows Rydberg SWM signals during dressing field detuning at a cell temperature of 60 °C, where each small peak in the figure represents an SWM signal. We fix the 780-nm laser wavelength at a chosen detuning and scan the 480-nm laser frequency to get the SWM signal. When the detuning of Δ_1 is 100 MHz, the SWM signal is the largest due to the electric field generated by the collisions of Rydberg atoms and Rydberg interaction, resulting in a Rydberg level shift, as explained in the theoretical section. Figure 4(b) shows only the envelope curves for 60 °C, 70 °C, and 80 °C. It shows that the 780-nm laser detuning for the maximum intensity of SWM signals changes with temperatures (corresponding ground-state atomic densities were N_1, N_2, and N_3). As the Rydberg interaction becomes strong and the ion density

increases, the intensity of SWM decreases, and the probe field detuning of the maximum SWM signal intensity increases. It is clear that probe field detuning with the maximum SWM signal intensity increased almost linearly as the temperature increased. Thus, to determine the electric field intensity induced by the ionization process, the experimental spectrum shift can be used to detect the ionization electric field by subtracting the calculated shift value caused by Rydberg interaction and comparing it to the calculated energy level shift results, as shown in Fig. 4(c).

4. Conclusion

In summary, we examined the characteristics of SWM spectra in the presence of Rydberg atom ionization and observed significant energy level shifts and broadening phenomena. The regulation and evolution patterns of SWM spectra are studied and analyzed in an ionized environment by varying the probe field power, principal quantum number, and atomic density. Theoretical calculations of field-induced energy level shifts revealed that the SWM spectrum of the Rydberg state can be used to measure ionizationinduced electric fields. These findings have important applications in the realm of electric field measurement based on the nonlinear spectrum of the atomic system.

Acknowledgements

Project supported by the Science and Technology Project of State Grid Corporation of China (Grant No. 5700-202355839A-4-3-WL). The authors sincerely thank Prof. Zhaoyang Zhang (Xi'an Jiaotong University) for providing the critical experimental datasets on Rydberg-state microwave responses.

References

[1] Gnedin Yu N, Mihajlov A A, Ignjatović Lj M, Sakan N M, Srećković V A, Zakharov M Yu, Bezuglov N N and Klycharev A N 2009 *New Astron. Rev.* **53** 259
[2] Zelener B B, Vilshanskaya E V, Saakyan S A, Sautenkov V A, Zelener B V and Fortov V E 2021 *JETP Lett.* **113** 82
[3] Gnedin Yu N, Mihajlov A A, Ignjatović Lj M, Sakan N M, Srećković V A, Zakharov M Yu, Bezuglov N N and Klycharev A N 2009 *New Astron. Rev.* **53** 259
[4] Hogan S D 2021 *Physics* **14** 145
[5] Wehrli D, Génévriez M, Knecht S, Reiher M and Merkt F 2021 *J. Phys. Chem. A* **125** 6681
[6] Letunov A Y and Lisitsa V S 2023 *Atoms* **11** 133
[7] Yuan J P, Yang W G, Jing M Y, Zhang H, Jiao Y C, Li W B, Zhang L J, Xiao L T and Jia S T 2023 *Rep. Prog. Phys.* **86** 106001
[8] Gallagher T F 1988 *Rep. Prog. Phys.* **51** 143
[9] Kastberg A 2020 *Structure of Multielectron Atoms* (Springer Nature Link)
[10] Jing M Y, Hu Y, Ma J, Zhang H, Zhang L J, Xiao L T and Jia S T 2020 *Nat. Phys.* **16** 911
[11] Zheng H B, Yao X, Zhang Z Y, Che J L, Zhang Y Q, Zhang Y P and Xiao M 2014 *Laser Phys.* **224** 045404
[12] Che J L, Ma J Q, Zheng H B, Zhang Z Y, Yao X, Zhang Y Q, Zhang Y P 2015 *Europhys. Lett.* **109** 33001
[13] Zhang Y P and Xiao M 2007 *Appl. Phys. Lett.* **90** 111104
[14] Zhang Y P, Brown A W and Xiao M 2007 *Phys. Rev. Lett.* **99** 123603
[15] Nie Z Q, Zheng H B, Li P Z, Yang Y M, Zhang Y P and Xiao M 2008 *Phys. Rev. A* **77** 063829
[16] Tong D, Farooqi S M, Stanojevic J, Krishnan S, Zhang Y P and Côté R, Eyler E E, Gould P L 2004 *Phys. Rev. Lett.* **93** 063001
[17] Ding D S, Busche H, Shi B S, Guo G C and Adams C S 2020 *Phys. Rev. X* **10** 021023
[18] Šibalić N, Pritchard J D, Adams C S and Weatherill K J 2017 *Comput. Phys. Commun.* **220** 319
[19] Weller D, Shaffer J P, Pfau T, Löw R and Kübler H 2019 *Phys. Rev. A* **99** 043418
[20] Nagesha K and MacAdam K B 2003 *Phys. Rev. Lett.* **91** 113202
[21] Deutsch H, MacAdam K B, Becker K, Zhang H and Märk T D 2005 *J. Phys. B* **39** 343
[22] Weller D, Urvoy A, Rico A, Löw R, Kübler H 2016 *Phys. Rev. A* **94** 063820
[23] Kramers H A 1923 *Philos. Mag.* **46** 836
[24] Anderson D A, Raithel G, Simons M and Holloway C L 2017 *arXiv* **1172** 08717
[25] Taylor D R 1978 *Can. J. Phys.* **56** 1308
[26] Zimmerman M L, Littman M G, Kash M M and Kleppner D 1979 *Phys. Rev. A* **20** 2251
[27] Wang X, He J, Bai J D and Wang J M 2020 *Appl. Sci.* **10** 5646